Technical Sciences, 2016, 19(4), 339–357

Quarterly peer-reviewed scientific journal
ISSN 1505-4675
e-ISSN 2083-4527
TECHNICAL SCIENCES
Homepage: www.uwm.edu.pl/techsci/

FLEXURAL BEHAVIOUR OF CONCRETE SLABS REINFORCED WITH FRP BARS IN EXPERIMENTS AND ACCORDING TO ACI 440.1R GUIDE

***Marcin Abramski*[1], *Piotr Korzeniowski*[2], *Witold Tisler*[3]**

[1] Department of Rail Transportation and Bridges
[2] Department of Concrete Structures
[3] Department of Geotechnics, Geology and Marine Civil Engineering
Faculty of Civil and Environmental Engineering
Gdansk University of Technology

Received 20 April 2016; Accepted 11 November 2016; Available online 21 November 2016

Key words: basalt fibres, carbon fibres, FRP reinforcement, reinforcement bar, concrete slab, experiment.

Abstract

The paper presents research conducted on two concrete slabs reinforced with the carbon composite bars and two other concrete slabs reinforced with basalt composite bars. The carbon bars were plain, while the basalt ones were ribbed. The slabs were experimentally investigated in the flexural state of effort with the concentrated forces applied. The results are compared with the analytical solution proposed in the guide ACI 440.1R-06 of the American Concrete Institute. The calculation procedures in respect of flexure, as well as deflection, as per ACI 440.1R-06, are presented, briefly explained and discussed in the paper. Some suggestions to revise the existing procedures are offered. The authors present and discuss the following results of their experimental investigation: the ultimate capacity of the slabs, their modes of failure, deflections and the strains in reinforcement.

Introduction

Using Fibre Reinforced Polymer (FRP) materials in concrete structures may be profitable for its durability. Apart from the high corrosion resistance there are other important advantages of FRP materials: magnetic neutrality

Correspondence: Marcin Abramski, Katedra Transportu Szynowego i Mostów, Politechnika Gdańska, ul. Narutowicza 11/12, 80-233 Gdańsk, phone: 58 347 18 38, e-mail: marcin.abramski@wilis.pg.gda.pl

and high tensile strength. Unfortunately, FRP have also its disadvantages in comparison to steel such as the fragility or the low elastic modulus which is (with the exception of carbon FRP) much lower than for steel. Moreover the FRP materials are not ductile at all: they do not yield but are elastic until the destruction. FRP materials are also anisotropic: they are strong to tension only in one direction. The behaviour of concrete reinforced with FRP reinforcement bars is different from a traditionally (i.e. with steel bars) reinforced structure. Application of this technology in construction requires from engineers a broadened knowledge on calculating load-carrying capacity of structures reinforced with FRP bars. This knowledge should be based on existing design standards.

The article presents research conducted on two concrete slabs reinforced with carbon composite bars and two other concrete slabs reinforced with basalt composite bars. The slabs were experimentally investigated in the flexural state of effort with concentrated forces applied.

One of the objectives of the experiments was to compare the behaviour of the slabs reinforced with the polymer bars made from the different fibres (basalt and carbon). The prices of the FRP bars are about seven times higher for the carbon composite than for the basalt composite. The authors preferred the ribbed bars as the reinforcement for the examined slabs. However the ribbed rods made from the carbon fibres were not available at the time. Consequently, the ribbed basalt bars and the plane carbon bars had to be used for the experiments.

The second objective was to compare the experimental load bearing capacity of the tested slabs with the analytical solution proposed in a guide (ACI 2006) of the American Concrete Institute.

State of the art

Flexural behaviour of concrete slabs reinforced with FRP bars is a very popular issue in recent years (SALAKAWY, KASSEM 2003), (GANGARAO et al. 2007). An intense research is carried out in China and Japan (SALAKAWY, KASSEM 2003) and in Europe (OSPINA and NANNI 2007), (EL-GHANDOUR et al. 2003). Experiments from the last few years show that FRP reinforcement bars have under some specific circumstances more advantages than traditional steel (SALAKAWY, KASSEM 2003).

As it is reported in the literature using FRP reinforcement instead of steel usually increases load capacity of a concrete slab. That is caused mainly due to high tensile strength of the FRP reinforcement. This fact is a very important argument for applying the alternative type of reinforcement. Using the same

amount of reinforcement a higher flexural strength (even up to 100%) can be obtained (SALAKAWY, KASSEM 2003). However, numerous differences between steel and FRP materials must be taken into account. Linear-elastic behaviour of FRP until failure, low ductility and lower elastic modulus than steel (with the exception of the carbon FRP) cause that load-carrying capacity of the concrete slab differs substantially. Concrete slab reinforced with steel bars usually achieves yield strength before rupture and failure is not rapid. Concrete slab reinforced with FRP bars are characterized by a different destruction mode: usually concrete crushing or rarely reinforcement rupture. The both failure modes are rapid.

The basalt FRP are an interesting alternative for the better known and wider spread carbon or glass FRP. In addition to good mechanical properties, basalt has a high chemical and thermal stability, good thermal insulating, electrical and sound properties. Basalt fibres are also significantly better chemically resistant than glass fibres, particularly in a strongly alkaline environment. For example, corrosive liquids and gases can be transported with pipes made of basalt composite (URBAŃSKI et al. 2013), (VAN DE VELDE et al. 2002).

The authors of the paper decided to program their experimental research based on the Guide for the Design and Construction of Structural Concrete Reinforced with FRP Bars (ACI 2006) published by the American Concrete Institute. Computations of a cross section strength according to that document should be based on the following assumptions:

– perfect bond exists between concrete and FRP reinforcement,

– the tensile behaviour of the FRP reinforcement is linearly elastic until failure,

– the tensile strength of concrete is ignored,

– the maximum usable compressive strain in the concrete is assumed to be 0,003,

– strain in the concrete and in the FRP reinforcement is proportional to the distance from the neutral axis.

Calculation procedures proposed by ACI 440.1R-06

Flexure

The strength design philosophy states that the design flexural capacity $\phi \cdot M_n$ must exceed the factored acting bending moment M_u:

$$\phi \cdot M_n \geq M_u \tag{1}$$

where:
M_n – nominal moment capacity,
M_u – factored moment at section,
ϕ – strength reduction factor.

The design flexural strength is calculated as nominal flexural strength M_n multiplied by a strength reduction factor ϕ. The nominal flexural strength is determined based on strain compatibility, internal force equilibrium and the controlled mode of failure.

In the beginning of the procedure a mode of failure has to be determined. A reinforcement ratio (Eq-2) has to be assumed and compared to the balanced reinforcement ratio (Eq-3). Comparison of these two values determine the failure mode. As it was mentioned above, FRP reinforcement does not yield, so balanced ratio is computed using design tensile strength:

$$\rho_f = \frac{A_f}{b \cdot d} \tag{2}$$

$$\phi_{fb} = 0.85 \cdot \beta_1 \cdot \frac{f_c'}{f_{fu}} \cdot \frac{E_f \cdot \varepsilon_{cu}}{E_f \cdot \varepsilon_{cu} + f_{fu}} \tag{3}$$

where:
ρ_f – FRP reinforcement ratio,
A_f – area of FRP reinforcement,
b – width of rectangular section,
d – distance from extreme compression fiber to centroid of tension reinforcement,
ρ_{fb} – FRP reinforcement ratio producing balanced strain conditions,
β_1 – factor reducing the real depth of the section, taken as 0.85 for concrete strength f_c' up to and including 4000 psi (28 MPa),
f_c' – specified compressive strength of concrete,
f_{fu} – design tensile strength of FRP, considering reductions for service environment,
E_f – design modulus of elasticity of FRP,
ε_{cu} – ultimate strain in concrete.

If the balanced ratio is bigger than reinforcement ratio ($\rho_{fb} > \rho_f$), the concrete crushing must be obtained. Otherwise, reinforcement rupture governs. In the following paragraph the case of concrete crushing is considered.

Based on the equilibrium of forces and strain compatibility (Fig. 1), it can be written as follows:

$$M_n = A_f \cdot f_f \cdot \left(d - \frac{a}{2}\right) \tag{4}$$

$$a = \frac{A_f \cdot f_f}{0.85 \cdot f_c' \cdot b} \tag{5}$$

$$f_f = E_f \cdot \varepsilon_{cu} \cdot \frac{\beta_1 \cdot d - a}{a} \tag{6}$$

where:
f_f – stress in FRP reinforcement in tension,
a – depth of equivalent rectangular stress block, equal $\beta_1 \cdot c$.

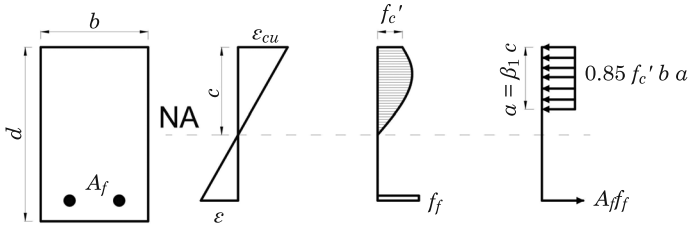

Fig. 1. Strain and stress distribution at ultimate conditions
Source: ACI (2006).

Substituting value a from equation (5) into equation (6), it can be obtained:

$$f_f = \left(\sqrt{\frac{(E_f \cdot \varepsilon_{cu})^2}{4} + 0.85 \cdot \beta_1 \cdot \frac{f_c'}{\rho_f} \cdot E_f \cdot \varepsilon_{cu}} - 0.5 \cdot E_f \cdot \varepsilon_{cu}\right) \leq f_{fu} \tag{7}$$

Nominal flexural strength is defined above. The FRP reinforcement is linearly elastic up to failure, so result of equation (7) must be less than f_{fu} (design tensile strength). This model of failure (concrete crushing) is recommended to design.

If $\rho_f < \rho_{fb}$ the failure mode is reinforcement rupture and maximum strain in concrete (0.003) may not be attained. The calculation procedure is other than for concrete crushing failure mode. Analysis has two unknown values: com-

pressive strain ε_c in concrete at failure and the depth to neutral axis c. Nominal flexural strength can be computed using equation (8):

$$M_n = A_f \cdot f_{fu} \cdot \left(d - \frac{\beta_1 \cdot c}{2}\right) \tag{8}$$

where:
c – distance from extreme compression fibre to the neutral axis.

For a given section the product of $\beta_1 \cdot c$ in equation above depends on material properties and FRP reinforcement ratio. The maximum value is obtained when maximum concrete strain (0.003) is attained. A simplified calculation of nominal strength is based on these two equations:

$$M_n = A_f \cdot f_{fu} \cdot \left(d - \frac{\beta_1 \cdot c_b}{2}\right) \tag{9}$$

$$c_b = \frac{\varepsilon_{cu}}{\varepsilon_{cu} + \varepsilon_{fu}} \cdot d \tag{10}$$

where:
c_b – distance from extreme compression fibre to centroid of tension reinforcement,
ε_{fu} – design rupture strain of FRP reinforcement.

Because FRP bars are not characterized by a ductile behaviour, a strength reduction factor must be used to provide a higher reserve of strength in a designed structural member. The strength reduction factor ϕ for compression controlled failure is 0.65 in recommendation (ACI 2006). The member constructed for concrete crushing may not fail accordingly. For instance, if the concrete strength is higher than specified, a member failure mode may be a FRP rupture. This is the main reason for creating a relationship between two values of factor ϕ. A section controlled by a concrete crushing is defined as a section in which $\rho_f > 1.4 \cdot \rho_{fb}$ and a section with FRP rupture is defined by $\rho_f > \rho_{fb}$. Strength reduction factor can be computed using equation (11):

$$\phi = \left\{ \begin{array}{c} 0.55 \text{ for } \rho_f < \rho_{fb} \\ 0.3 + 0.25 \cdot \frac{\rho_f}{\rho_{fb}} \text{ for } \rho_{fb} \le \rho_f < 1.4 \cdot \rho_{fb} \\ 0.65 \text{ for } \rho_f \ge 1.4 \cdot \rho_{fb} \end{array} \right\} \tag{11}$$

A relation between strength reduction factor and reinforcement ratio is presented on Fig. 2. There is a linear transition between factors 0.55 and 0.65.

If a member is designed to fail by FRP rupture, a minimum amount of reinforcement should be obtained ($\phi \cdot M_n \geq M_{cr}$). Provisions are based on ACI 318-14 (American Concrete Institute 2014). To compute a minimal amount of reinforcement eq. (12) can be used.

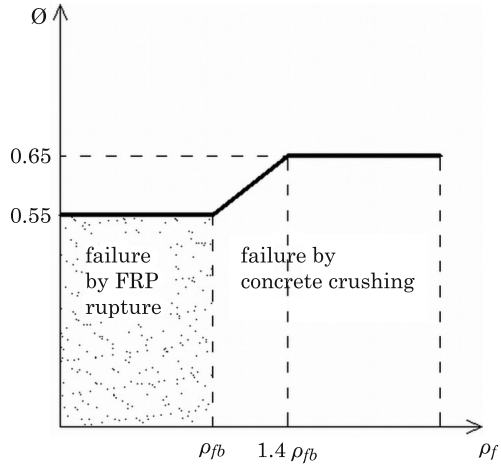

Fig. 2. Strength reduction factor as a function of the reinforcement ratio
Source: ACI (2006).

$$A_{f,\min} = \frac{4.9 \cdot \sqrt{f_c'}}{f_{fu}} \cdot b_w \cdot d \geq \frac{330}{f_{fu}} \cdot b_w \cdot d \tag{12}$$

where:

$A_{f,\min}$ – minimum area of FRP reinforcement needed to prevent a failure of flexural member upon cracking,

b_w – width of the web.

If a failure mode is concrete crushing ($\rho_{fb} > \rho_f$) the minimum amount of reinforcement is automatically achieved. Therefore, eq. (12) can be used only if failure mode is controlled by FRP rupture.

Deflection

Calculating the short term deflection in the ACI Report (ACI 2006) is based on the effective moment of inertia. Taking into consideration the differences in stiffness and bond characteristic between steel and FRP, an effective moment of inertia is computed using the following equation:

$$I_e = \left(\frac{M_{cr}}{M_a}\right)^3 \cdot I_g \cdot \beta_d + \left[1 - \left(\frac{M_{cr}}{M_a}\right)^3\right] \cdot I_{cr} \leq I_g \tag{13}$$

where:
I_e – effective moment of inertia,
β_d – reduction coefficient used in calculating deflection,
M_{cr} and M_a – cracking and applied moment, respectively,
I_{cr} and I_g – cracked and gross moment of inertia of concrete section, respectively.

The most important factor in this equation is β_d which reduces the stiffness of FRP bars. In the next to last revision of ACI (ACI 2003) this coefficient was based on the proportion of the FRP and steel elastic moduli:

$$\beta_d = 0.5 \cdot \left(\frac{E_{\text{FRP}}}{E_s} + 1\right) \tag{14}$$

where:
E_{FRP} – modulus of elasticity of FRP.

However effective moment of inertia I_e calculated with use of the equations (13) and (14) resulted in obtaining too low values of deflection. Therefore coefficient β_d required some new considerations. The newer evaluation of FRP RC test data, based on (YOST et al. 2003), leads to the following proposal:

$$\beta_d = \frac{1}{5} \cdot \frac{\rho_f}{\rho_{fb}} \leq 1 \tag{15}$$

Based on the value of effective moment of inertia a deflection of a simply supported beam can be computed using the following equation:

$$\Delta = \frac{5}{48} \cdot \frac{M \cdot l^2}{E_c \cdot I_e} \tag{16}$$

where:
Δ – deflection due to sustained loads,
M – maximum bending moment,
l – span length,
E_c – modulus of elasticity of concrete.

Analysing the two β_d approaches two values of deflection can be obtained, one with coefficient used in the previous guide (ACI 2003) and second – in the current one (ACI 2006). The authors performed a comparative analysis of the both approaches (Tab. 1). Material characteristics of concrete, amount of

reinforcement and the applied moment (which was assumed as equal to 20 kNm) are the same for all cases. Moduli of elasticity and ultimate tensile strengths of reinforcement are taken from the report (ACI 2006).

Table 1

Comparison of different approaches to calculating β_d coefficient

Type of reinforcement	Modulus of elasticity E_f [GPa]	Ultimate tensile strength f_{fu} [MPa]	Coefficient (eq. 15) β_1 [–]	Coefficient (eq. 14) β_2 [–]	Moment of inertia (eq. 13) I_{e1} mm^4	Moment of inertia (eq. 13) I_{e2} mm^4	Deflection (eq. 16) Δ_1 mm	Deflection (eq. 16) Δ_2 mm
GFRP	41.4	552	0.262	1.530	$2.99 \cdot 10^6$	$3.2 \cdot 10^6$	53.1	49.58
AFRP	82.7	1172	0.584	2.568	$5.46 \cdot 10^6$	$5.79 \cdot 10^6$	29.04	27.38
CFRP	152	2070	1.000	4.300	$9.0 \cdot 10^6$	$9.55 \cdot 10^6$	17.62	16.61

Authors' experimental investigation

Four slabs were experimentally investigated. Two slabs were reinforced with basalt FRP bars and two other with carbon FRP bars. The slabs were 360 cm long × 90 cm wide × 8 cm thick and had two spans, both 160 cm long (Fig. 3).

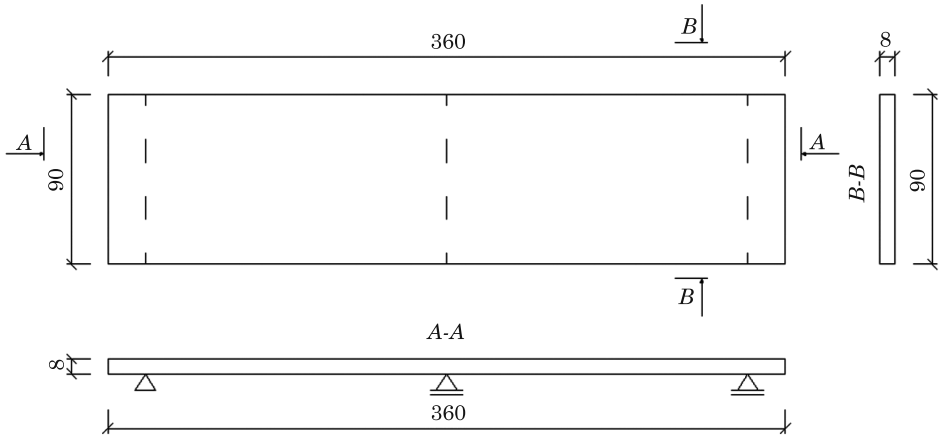

Fig. 3. Dimensions of the investigated slabs

Test specimens and material properties

The diameters of the both bar types were equal to 8 mm. The basalt bars were ribbed while the carbon bars were plane (as mentioned beforehand, the ribbed carbon bars were unavailable). The ribs in the basalt bars were made by

winding the additional basalt yarn around the previously prepared plane bars, see Figure 4.

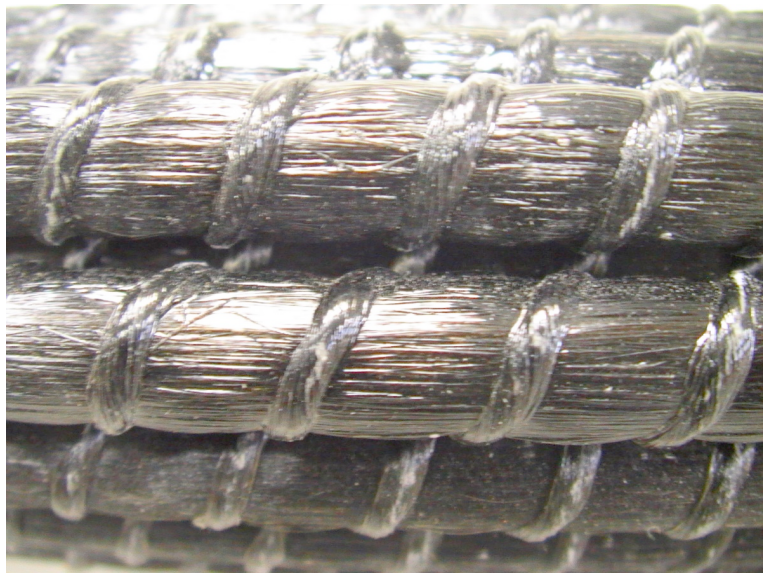

Fig. 4. Detail of basalt FRP bars

Parameters of the slabs and concrete are presented in Table 2.

An amount of reinforcement was the same in all investigated slabs. The reinforcement ratio was bigger than the balanced ratio ρ_{fb}. The expected mode of failure was mostly the concrete crushing. Configuration of the reinforcement was a little different in the both slab types (Tab. 3, Fig. 6). For all the slabs concrete cover was 1.5 cm both at the top and the bottom. The material characteristics declared by suppliers were similar for the both bar types. An important difference was a surface of the bars. The basalt bars were ribbed on their entire length and the carbon bars were plain. This fact influenced the experiments results very much.

Table 2

Material characteristics

Bar type		Reinforcement (according to supplier data)		Concrete (according to results of the own tests)	
		tensile strength [MPa]	elastic modulus [GPa]	compressive strength [MPa]	elastic modulus [GPa]
Basalt FRP	B-1	1100	90	37.88	34.98
	B-2	1100	90	37.88	34.98
Carbon FRP	C-1	1280	98	34.78	36.60
	C-2	1280	98	35.70	37.40

Table 3

Details of slab reinforcement at their bottom and top sides

SLAB		ρ_f [%]	ρ_{fb} [%]	ρ_f/ρ_{fb} [%]	Bars positioning			
					number on top	length [cm] in the both sides from the central support	number at the bottom	length
BASALT	B-1	0.94	0.73	1.29	11	50	11	whole slab
	B-2	0.94	0.73	1.29	11	40	11	whole slab
CARBON	C-1	0.94	0.55	1.73	11	100	11	whole slab
	C-2	0.94	0.56	1.69	11	100	11	whole slab

Test set-up

The slabs were loaded by two equal concentrated forces (Fig. 5). The load was controlled by displacement.

Fifteen strain gauges were installed on each slab, 9 on the top reinforcement and 6 in bottom reinforcement (Fig. 6). Arrangement of strain gauges at the top reinforcement was intentionally asymmetrical towards an axis of the middle support. The distance between the axis and the strain gauges in the left span was L/3 (where L was 1.6 m – span length). At the right span this distance was equal to L/4.

Two indicators were used to measure a deflection of the slab. The indicators were installed at one edge of the slab, directly underneath the points, were two concentrated forces acted. The accuracy of the measurement was equal to 0,01 mm. The left span of the slab has been marked as the *W* (the point of the compass) and the right one as *E*.

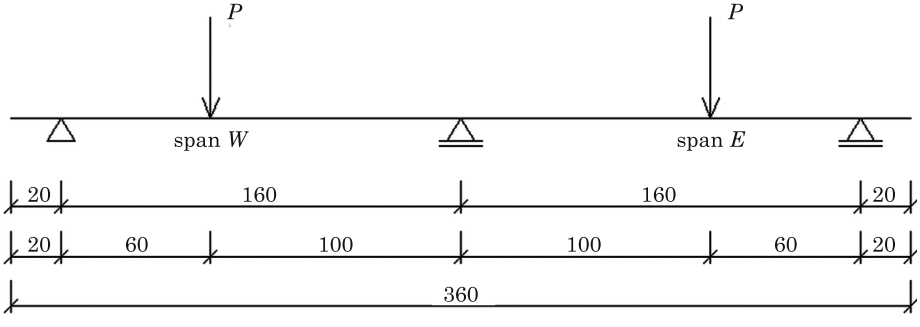

Fig. 5. Static scheme of experimental set-up

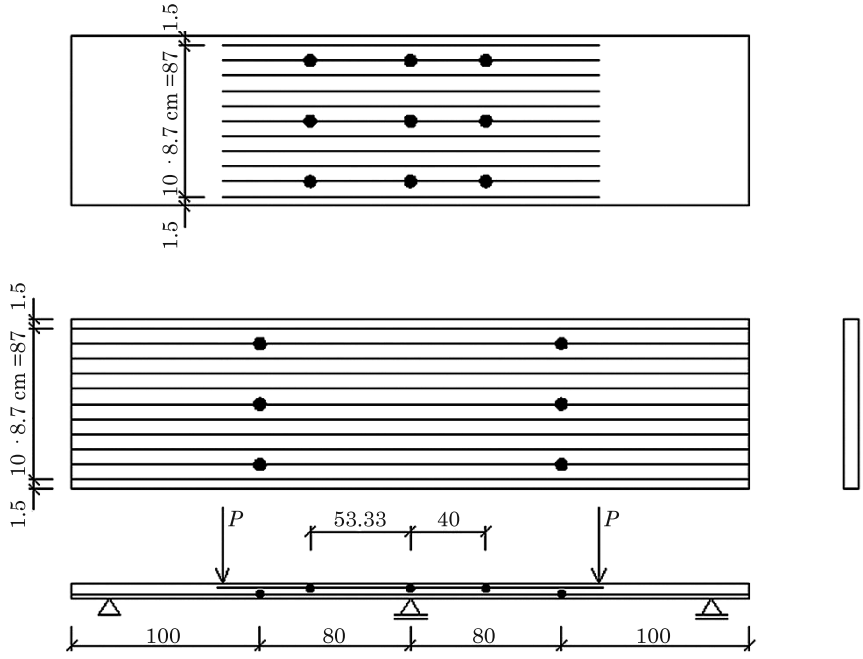

Fig. 6. Location of strain gauges

Test results and discussion

Ultimate capacity and mode of failure

The amount of reinforcement was the same in every investigated slab. The calculation based on a procedure proposed by ACI guide (ACI 2006) brought a concrete crushing as an expected failure mode, because reinforcement ratio ρ_f was 1.78 times higher than balanced reinforcement ratio ρ_{fb}.

In the case of the slabs reinforced with the basalt bars the failure mode was as expected, the same as in the over-reinforced slabs with the steel reinforcement, see Figure 7.

Unexpectedly, the failure mode of slabs reinforced with carbon bars was definitely different. The most probable reason for that was a weak bond between concrete and bars. As a result, the obtained load-carrying capacities of the slabs C-1 and C-2 were significantly lower than expected and reached 40% of the calculated value, i.e. 90 kN (see Tab. 4). Three splits were formed: one in the symmetry axis of the elements and two under the point loads (Fig. 8). All the splits developed before the destruction of the slabs. The reason for the premature failure must have been slip of reinforcement bars in concrete. The

Fig. 7. Slab B-2 shortly before its failure

carbon bars were plain, while the basalt ones were ribbed. The slip hypothesis was confirmed by the behaviour of the longitudinal reinforcement bars. They were not covered by concrete at the slab face and were visible on two face surfaces of the slab before the test beginning. When the experiments were over, the bars were visible too, but they were pulled about 1 cm into the slab (Fig. 9).

Table 4

Comparison of test results with code predictions

Type of reinforcement		Experimental failure load [kN]	Theoretical flexural capacity [kN]	Experimental/ Theoretical [–]	Experimental/ Theoretical with strength reduction factor (0.65) [–]	Mode of failure
BASALT	B-1	70	91.46	0.765	1.17	CC
	B-2	65	91.46	0.71	1.10	CC
CARBON	C-1	35	89.36	0.39	0.60	SF
	C-2	38	90.86	0.42	0.64	SF

Note: CC – failure obtained by the concrete crushing
SF – failure obtained by the reinforcement slip in concrete.

Fig. 8. Mode of failure slabs C-1 and C-2

Fig. 9. Detail of slab C-2 after its failure

In the Table 4 the predicted values of load-carrying capacities of the tested slabs are compared with the experimental results. The predicted values were computed based on the calculation procedures presented in the chapter 3. The strength reduction factor ϕ was taken into account according to the equation (11). It is worth noting that in the case of the slabs reinforced with the carbon plain bars the predicted load-bearing capacity is much overestimated in comparison to the experimental one. Such a difference is not acceptable. In the case of the slabs reinforced with the ribbed basalt bars the

load-bearing capacity obtained from the experiments is much lower than the theoretical value, but when the strength reduction factor ϕ is used, the consistency between experimental and theoretical load-bearing capacity is quite good (does not exceed 17%).

The obtained difference in the load-carrying capacities of the both slab types was equal up to 50% (Fig. 10).

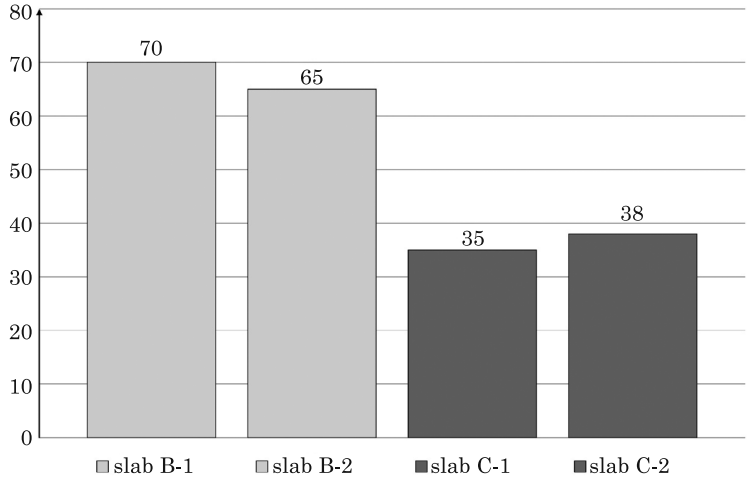

Fig. 10. Load-carrying capacities in [kN] of the tested slabs

Deflection

The load versus deflection diagrams for all the tested slabs are presented in Figure 11. The deflection was taken as the mean value from the both spans. All the slabs reached deflection of about 4 cm. The cracking bending moment was observed for all the slabs at the load level 15 kN.

The load-deflection curves obtained for the slabs reinforced with bars made of basalt composite (B-1 and B-2) differ considerably from the curves obtained for the slabs reinforced with bars made of carbon composite (C-1 and C-2). The first two curves are almost bilinear: they consist of two almost straight sections: before cracking and after cracking up to failure. In case of the slabs C-1 and C-2 the second section of the curve becomes flat shortly before reaching the maximum load level. The reason of such a behaviour must be a slip of plain carbon bars in concrete.

None of experimental curves coincide in the stage after cracking with a development of deflection obtained analytically according to (ACI 2006). The deflections obtained analytically are too small in comparison to experimental

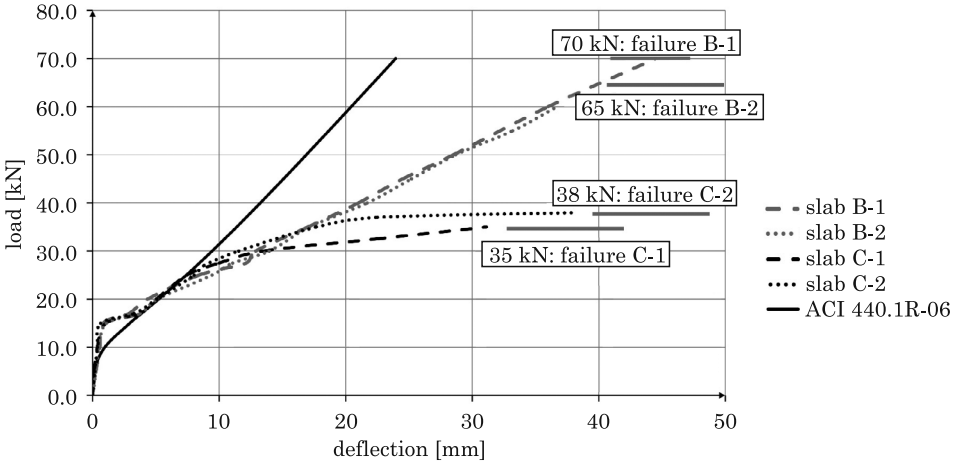

Fig. 11. Load versus deflection diagrams obtained in four experiments and in an analysis performed according to (ACI 2006)

data. The reason of this inconsistency is factor β_d (Eq. 15). According to the last version of the guidelines (ACI 2006) this factor depends on the balanced reinforcement ratio ρ_{fb}. This ratio is influenced by the ultimate tensile strength f_{fu} (Eq. 3). It means that deflection could be different for elements which have the same stiffness but different ultimate strength, which is incorrect. This remark was noticed already in (EL-GHANDOUR et al. 2003) and was recommended to consider in the next revision of the guidelines (ACI 2006).

According to the previous version of (ACI 2006) the factor β_d was computed according to equation (14), which was giving much higher values. The application of that approach leads to increasing effective moment of inertia I_e and would in effect result in even lower deflections that obtained from equation (15). It confirms, that the changes made in the last revision of the guidelines (ACI 2006) were needed.

Strains in reinforcement

Figures 12 and 13 present strain development in the reinforcement bars under the concentrated loads (Fig. 12) and in the symmetry axis of the slab (Fig. 13) versus the applied load. The graphs made for the slabs with basalt reinforcement do not present the full range of loading the slabs because of local damages of strain gauges. The damages occurred by strain level of about 6%.

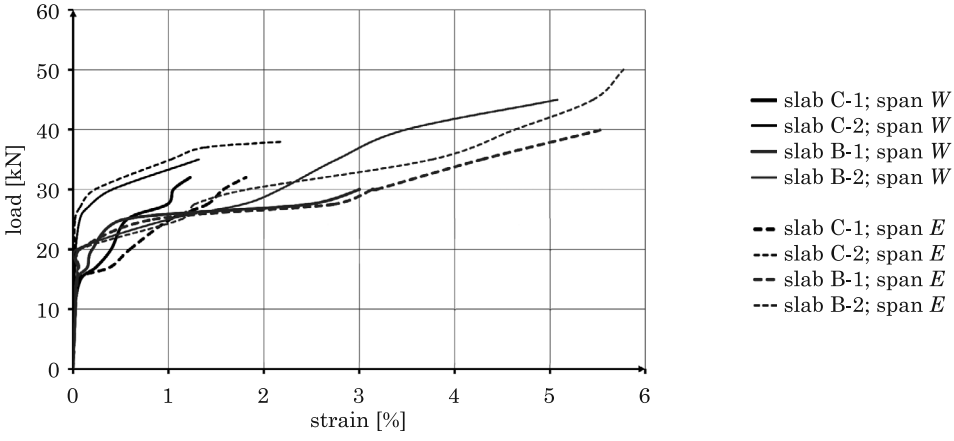

Fig. 12. Comparison of strain development in all the tested slabs in the both spans: *W* and *E*

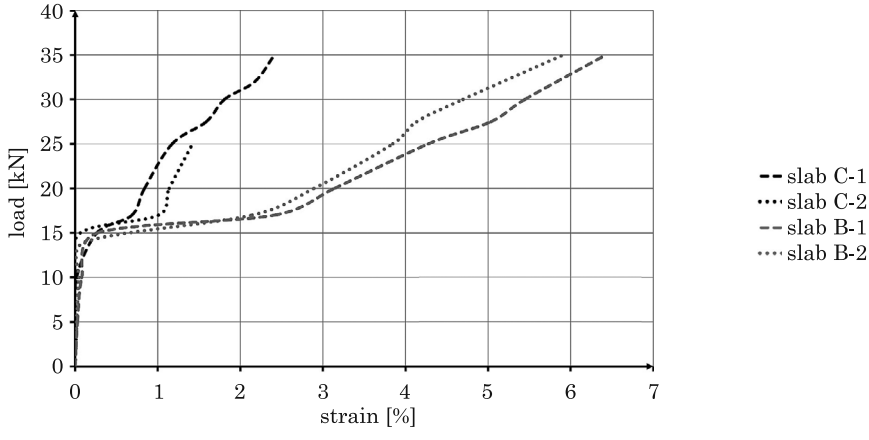

Fig. 13. Comparison of strain development in the symmetry axis of the slab (i.e. over the middle support)

If properly anchored, the both basalt and carbon bars would have been deformed longitudinally to the same extent up to load level $P = 30$ kN, as the deflection development up to that load level was very similar for all the tested slabs (see Fig. 11). However, the strain development in carbon bars was slow in comparison to basalt bars. Therefore, the reinforcement bars made of carbon composite were significantly less effective. In case of the slab C-2 the lower effectiveness was observed since the cracking load ($P = 15$ kN) up to failure ($P = 38$ kN). In case of the slab C1 it was observed also since the cracking load ($P = 15$ kN) for the support bars and since the load level about $P = 25$ kN for the bars of the both spans. The strain development presented in the both diagrams confirms the slip of carbon bars in concrete.

Conclusions

As mentioned beforehand the objective of the authors' investigations was to compare the behaviour of the concrete slabs reinforced with the basalt and carbon bars, whereas it turned out that the crucial problem was not in the material of the fibres but in the bond between the concrete and the polymer bars. Load-carrying capacity of slabs reinforced with ribbed bars is definitely higher than capacity of slabs reinforced with plain ones, although the strength as well as the modulus of the elasticity were higher for the plain carbon bars than for the ribbed basalt ones. In the presented experimental investigation the difference was equal to 50%. The plain bars (in the presented investigation made of a carbon composite) cannot be properly anchored in concrete and are not effective in sustaining bending moments. The problem of the bond between the concrete and the bar seems to be crucial when using the polymer bars as a reinforcement of the concrete structures. The surface of the plain polymer bars should be made rough, for instance by coating it with special adhesive and sand. The American guidelines (ACI 2006) address this problem just in an outline. Thus, the calculation procedures proposed by this guide is not useful if a bond between FRP reinforcement and concrete is too weak, like in the case of plain bars. In such a case the flexural failure mode differs much from the mode assumed in the theory of reinforced concrete structures.

In case of slabs reinforced with ribbed bars (in the presented investigation made of a basalt composite) the load-carrying capacity calculated according to (ACI 2006) is more consistent with the experimental results. However, deflections obtained from the calculation procedure underestimate the values obtained in the experiments. The problem was reported in the literature (EL-GHANDOUR et al. 2003) and should be considered in the next revision of the guidelines.

Acknowledgement

The research was co-financed by the European Union from the European Regional Development Fund (85%) and by Polish Ministry of Regional Development (15%) as part of operational programme "Innovative Economy". The project was called "Innovative means and effective methods to improve safety and durability of buildings and transport infrastructure in a sustainable development strategy" and was run by Technical University of Lodz, Poland. The authors of this paper carried out Task No. 018818. This support is greatly acknowledged.

References

ACI. 2003. *Guide for the Design and Construction of Concrete Reinforced with FRP Bars*. ACI 440.1R-03.

ACI. 2006. *Guide for the Design and Construction of Structural Concrete Reinforced with FRP Bars*. ACI 440.1R-06.

American Concrete Institute. 2014. *Building code requirements for structural concrete and commentary*. ACI 318-14, p.525.

El-Ghandour A.W., Pilakoutas K., Waldron P. 2003. *Punching Shear Behavior of FRP RC Flat Slabs* Part 1: *Experimental Study*. Journal of Composites for Construction, 7(3): 258–265.

Gangarao H.V.S., Taly N., Vijay P.V. 2007. *Reinforced Concrete Design with FRP Composites*. Boca Raton, Florida, USA: CRC Press.

Ospina C.E., Nanni A. 2007. *Current FRP-reinforced concrete design trends in ACI 440.1 R*. Proceedings of the 8th International Symposium on Fiber Reinforced Polymer Reinforcement for Concrete Structures – FRPRCS-8. Patras, Greece, pp. 14–6.

El-Salakawy E., Kassem C., Benmokrane B. 2003. *Flexural behaviour of bridge deck slabs reinforced with FRP composite bars*. Proc., 6th International Symposium on FRP Reinforcement for Concrete Structures. Singapore. Singapore: World Scientific Publishing, pp. 1291–1300.

Urbański M., Łapko A., Garbacz A. 2013. *Investigation on concrete beams reinforced with basalt rebars as an effective alternative of conventional R/C structures*. 11th International Conference on Modern Building Materials, Structures and Techniques. Vilnius, Lithuania, pp. 1183–1191.

Velde Van De K., Kiekens P., Van Langenhove L., Cater S. 2002. *Basalt fibers as reinforcement for composites.* Editorial, International Composites News.

Yost J.R., Gross S.P., Dinehart D.W. 2003. *Effective Moment of Inertia for Glass Fiber-Reinforced Polymer-Reinforced Concrete Beams*. ACI Structural Journal, 100(6): 732–739.